Specific heat and optical birefringence of $Fe_{0.25}Zn_{0.75}F_2$

W. C. Barber and D. P. Belanger
Department of Physics, University of California, Santa Cruz, California 95064
(Received 15 November 1999)

The specific heat (C_m) and optical birefringence (Δn) for the magnetic percolation threshold system $Fe_{0.25}Zn_{0.75}F_2$ are analyzed with the aid of Monte Carlo (MC) simulations. Both Δn and the magnetic energy (U_m) are governed by a linear combination of near-neighbor spin-spin correlations, which we have determined for Δn using MC simulations modeled closely after the real system. Near a phase transition or when only one interaction dominates, the temperature derivative of the birefringence $[d(\Delta n)/dT]$ is expected to be proportional to C_m since all relevant correlations necessarily have the same temperature dependence. Such a proportionality does not hold for $Fe_{0.25}Zn_{0.75}F_2$ at low temperatures, however, indicating that neither condition above holds. MC results for this percolation system demonstrate that the shape of the temperature derivative of correlations associated with the frustrating third-nearest-neighbor interaction differs from that of the dominant second-nearest-neighbor interaction, accurately explaining the experimentally observed behavior quantitatively.

Measuring the linear optical birefringence (Δn) in anisotropic, antiferromagnetic crystals undergoing magnetic phase transitions is a powerful way of determining the magnetic specific-heat (C_m) critical behavior. It has been shown[1–3] that the temperature derivative of the optical birefringence $[d(\Delta n)/dT]$ is proportional to C_m. In many cases, the birefringence technique has provided the most precise experimental determinations of universal critical behavior parameters[4] in pure and randomly mixed and dilute magnetic Ising systems. For the case of the three-dimensional ($d=3$) random-field Ising model (RFIM), which applies for a dilute antiferromagnet with an applied field along the ordering direction, birefringence measurements yielded evidence of a phase transition.[5] The advantages of the technique are threefold: the technique is typically much easier to employ than traditional heat pulse techniques; the effects of concentration gradients inevitably present in mixed and dilute crystals can be greatly reduced;[3] and the phonon contributions to the specific heat are greatly suppressed in the birefringence. Since the transition typically varies with concentration in mixed and dilute systems, the critical behavior is often masked by the concentration gradients quenched into the system during growth. The laser beam used in the optical technique can be aligned perpendicular to the gradient, often reducing the gradient effects by an order of magnitude. This has been crucial in the study of random-exchange Ising model (REIM) and RFIM systems in $d=2$ and 3. The virtual elimination of the phonon background has allowed detailed analysis of the specific heat in $d=1$ and 2 systems. For $d=2$ this has allowed a detailed comparison[6] of the magnetic specific heat of the pure system and the Onsager solution to the $d=2$ Ising model and, for dilute systems, a scaling analysis of the destruction of the phase transition by random fields in the $d=2$ Ising model.[7] For $d=1$, the technique has been used successfully to determine the exchange constants in systems where the phonon background overwhelms the magnetic contributions to conventional specific-heat data.[8]

That C_m and $d(\Delta n)/dT$ are proportional in certain cases is a consequence of the fact that both Δn and the magnetic energy (U_m) are governed by a linear combination of near-neighbor spin-spin correlations.[2] This proportionality has been experimentally shown explicitly[9] for the $d=3$ pure Ising system FeF_2 as well as its site-diluted counterparts[10,11] $Fe_{0.93}Zn_{0.07}F_2$ and $Fe_{0.46}Zn_{0.54}F_2$ by comparing directly the pulsed heat and optical data. This proportionality has been demonstrated both in zero applied field ($H=0$) and in applied fields. The magnetically dilute crystals of $Fe_{1-x}Zn_xF_2$ have been the most extensively studied[4] realizations of the RFIM, an important class of systems with randomness and frustration. Such experimental verification has been crucial in this controversial field since some authors[12] have expressed reservations about the proportionality for $H>0$, i.e., the RFIM case.

Despite the experimental verification of the proportionality between C_m and $d(\Delta n)/dT$, it is important to verify the details of the mechanism for the proportionality near phase transitions in a specific case. One opportunity to analyze the detailed relationship between C_m and $d(\Delta n)/dT$ presents itself in the compound $Fe_{0.25}Zn_{0.75}F_2$, which, with respect to the dominant exchange interaction J_2 is at the magnetic percolation threshold, the concentration below which no ordering is possible. Throughout the rest of this work we will refer to the percolation threshold concentration as the appropriate one if only J_2 were being considered. The presence of other interactions make the concept of percolation more complicated and they can play an important role in the ordering processes even when they are very small. Interestingly, $d(\Delta n)/dT$ data for $Fe_{0.25}Zn_{0.75}F_2$ exhibit a change[13] in sign near $T=8$ K. While the high-temperature behavior of $d(\Delta n)/dT$ is accurately proportional to C_m, the sign reversal in $d(\Delta n)/dT$ at low temperature is not reflected, of course, by the behavior of C_m. We present data obtained from both the optical and pulsed heat techniques that show the nonproportionality between C_m and $d(\Delta n)/dT$ at low T, as shown in Fig. 1. We also present Monte Carlo (MC) simulation results that can be used to explain why the proportionality breaks down between C_m and $d(\Delta n)/dT$ at low tem-

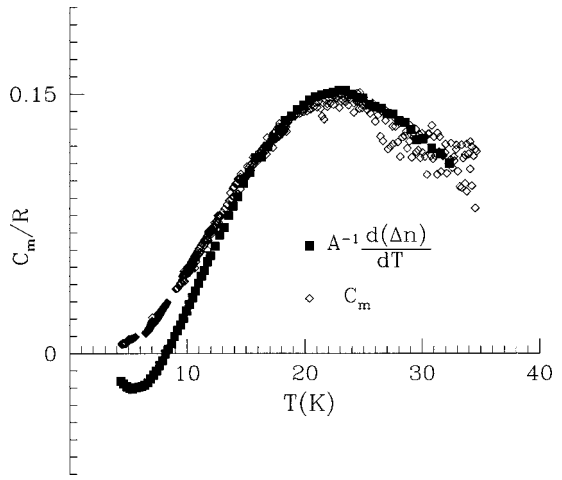

FIG. 1. The magnetic specific heat $C_m/R=C_p/R-B$, where B is the background, versus T for $Fe_{0.25}Zn_{0.75}F_2$. The phonon contribution to the specific heat has been subtracted as discussed in the text. Also shown is the temperature derivative of the birefringence $d(\Delta n)/dT$ versus T scaled with the proportionality found at other concentrations.

peratures. U_m and Δn each depend on the near-neighbor spin-spin correlations, but with different weights. We show that whereas U_m is dominated by the second-nearest-neighbor correlation, Δn is predominantly governed by the third-nearest-neighbor correlation that shows a different temperature dependence below 15 K. The results of this study are consistent with theory regarding the proportionality between C_m and $d(\Delta n)/dT$ near a phase transition, where the different spin-spin correlations must necessarily have the same temperature dependence. We also demonstrate that an applied field has a predictable effect on both U_m and Δn.

The compound $Fe_{1-x}Zn_xF_2$ is ideal for RFIM studies. Pure FeF_2 is well modeled by the Hamiltonian

$$\mathcal{H}=\sum_l \sum_{i<j} J_l \vec{S}_i \cdot \vec{S}_j + D\sum_i \vec{S}_i^2. \tag{1}$$

The $\vec{S}=2$ system has the interaction strengths $J_1=-0.069$ K, $J_2=5.278$ K, and $J_3=0.279$ K, as determined from neutron inelastic scattering measurements.[14] The large crystal-field anisotropy $D=9.29$ K persists while the exchange interactions remain largely constant as the magnetic spins are diluted[15] in $Fe_{1-x}Zn_xF_2$, making this an excellent Ising system for all magnetic concentrations x. Single crystals can be grown for all x with very small concentration gradients[16] and with superb structural quality. The magnetic interactions are dominated by the antiferromagnetic second-nearest-neighbor super-exchange interaction, J_2, between the body-center and body-corner ions. All other interactions are negligible except near the percolation threshold concentration, where a small frustration due to the third-nearest-neighbor interaction between ions of the same sublattice along the direction perpendicular to the spin-ordering c axis, J_3, becomes important.[17] At low temperatures, the Heisenberg character of the spin-spin interaction is less important and we might expect U_m to be fairly represented, for $H=0$, by the REIM Hamiltonian

$$\mathcal{H}=\sum_l \sum_{i<j} J_l \epsilon_i \epsilon_j S_i S_j, \tag{2}$$

where $S_i=\pm 2$, $\epsilon_i=1$ if site i is occupied and zero otherwise, and J_l is the strength of the lth nearest-neighbor interaction. C_m is then given by a sum of temperature derivatives of spin-spin correlations,

$$C_m=\frac{d(U_m)}{dT}=\sum_l \sum_{i<j} J_l \epsilon_i \epsilon_j \frac{d(\langle S_i S_j\rangle_l)}{dT}, \tag{3}$$

where the J_l are assumed independent of temperature. The temperature-dependent birefringence (Δn), the difference between the indices of refraction along the spin ordering axis and perpendicular to it, depends only on a linear combination of the same correlation functions. The temperature derivative yields

$$\frac{d(\Delta n)}{dT}=\sum_l \sum_{i<j} I_l \epsilon_i \epsilon_j \frac{d(\langle S_i S_j\rangle_l)}{dT}. \tag{4}$$

In general the values of the coefficients I_l associated with Δn are not related to the respective values J_l. Nevertheless, we will find a proportionality between C_m and $d(\Delta n)/dT$ in a temperature regime where the temperature dependence of the contributing correlations $\langle S_i S_j\rangle_l$ are all proportional. This is necessarily the case in the critical region of a phase transition where the correlation length grows larger than any relevant interaction length and all spin-spin correlations necessarily have the same temperature dependence. We may also find an excellent proportionality between C_m and Δn in the case where one magnetic interaction dominates in both C_m and $d(\Delta n)/dT$. Such is the case[3] of MnF_2, where the proportionality holds accurately over a very wide temperature range, $5<T<100$ K. A lack of proportionality has been observed in pseudo-low-dimensional systems[2,18] where neither of the above conditions holds. The percolation threshold presents another opportunity to observe a breakdown in proportionality between C_m and $d(\Delta n)/dT$, since small frustrating interactions can affect spins with few or no neighbors connected by the dominant exchange interaction. We will show that this is indeed the case for the percolation threshold sample $Fe_{0.25}Zn_{0.75}F_2$. We will also show that the behavior is readily interpreted using the results of MC simulations of this Ising antiferromagnet.

The $Fe_{0.25}Zn_{0.75}F_2$ crystal was cut from a boule grown[19] at the University of California, Santa Barbara. For the adiabatic heat pulse technique, the 2.24-g sample was mounted on a thin sapphire plate using GE7031 varnish. A small Stablohm 800 wire heater, connected to a four-wire constant-power supply, was wound and varnished onto the sapphire plate. A shielded carbon thermometer was attached with varnish to the sample and was connected using a four-wire technique to a current ratio transformer resistance bridge. The sample was suspended inside a sample chamber by 0.0254-mm Be-Cu wires used to connect to the thermometer and heater. While providing good electrical connections, the alloy wires provide only a small heat leak from the sample to the copper sample chamber. In this way, the heat generated by the thermometer leaks away from the sample in a way controlled by a temperature difference, δT, between the sample chamber

and the sample. In the absence of a heat pulse, the sample temperature can remain constant if δT is properly controlled. This is done by controlling δT with a bridge and controller using the sample thermometer and a thermometer located in a cold finger, commercially calibrated for $H=0$, upon which the sample chamber is mounted. A second thermometer in the cold finger is used with a second bridge to determine the absolute temperature. A preliminary calibration is performed to determine δT versus T such that the sample temperature does not drift in the absence of a heat pulse. The calibration is incorporated into computer control algorithms so that the balance is automatically preserved over the entire temperature range during a specific-heat experiment. The computer applies a pulse and determines the resulting change in temperature, from which the specific heat is calculated. The thermometry sensitivity is approximately 50 μK. The pulse energy ranged from approximately 3 μJ at the lowest temperatures to 8 mJ at the highest temperatures where measurements were made. After collecting specific-heat data for the sample and addenda, the sample is removed from the sample chamber and the thermometer is fixed to the sapphire plate. The specific heat of the thermometer, the sapphire plate, the varnish and the wires is then measured at $H=0$. This background specific heat is subtracted from all of the specific-heat data before further analysis. The phonon contribution to the total specific heat is approximated by the Debye model, valid at temperatures small relative to the Debye temperature. The Debye temperature[20] for pure nonmagnetic ZnF_2 is 250 K and that of FeF_2 is 256 K. We weighted the two pure Debye temperatures by the respective concentrations to obtain a Debye temperature of 252 K for $Fe_{0.25}Zn_{0.75}F_2$. The Debye specific heat is calculated with this Debye temperature and is subtracted from the data leaving the magnetic component of the specific heat (C_m) which can then be used in comparisons with Δn and MC results.

For the birefringence (Δn) measurements, two faces were polished parallel to the spin-ordering c axis. A linearly polarized laser beam ($\lambda=632.8$ nm) impinges normally upon the sample with a polarization 45° to the c axis. The beam traverses a distance of 8.05 mm through the sample. A 0.5 mm pinhole in front of the sample minimizes the effects of concentration gradients and vibrations. The Sénarmont technique is used to measure Δn with a resolution of 2×10^{-9}. Calibrated carbon resistance thermometers, used for their low-field dependence and high sensitivity, yield a temperature stability better than 50 μK. The sample was zero-field cooled (ZFC) to 5 K before slowly raising the temperature in approximately 0.1 K steps. About 400 s were required to establish equilibrium and to measure Δn at each step. Reasonable variations in the rates of heating and cooling and stabilization times had no observable effect on the data.

The correlation functions for the first three nearest-neighbor pairs have been calculated using MC simulations. The magnetic lattice corresponding to the body-centered-tetragonal $Fe_{1-x}Zn_xF_2$ lattice is described as two cubic sublattices of size $L\times L\times L$ each, delineated as one-dimensional arrays bit coded to accommodate large lattice sizes. All of the results reported here were obtained with $L=256$, corresponding to more than 3.3×10^7 sites magnetically occupied with probability x. Beginning at high temperature each magnetic site is randomly visited many times and flipped with a probability given by either the heat bath or metropolis algorithm in temperature steps of 0.01 K. Both periodic boundary conditions and free boundary conditions were applied to the lattices as they were cooled and then warmed in magnetic fields of $H=0$ and 2 T. The first three nearest-neighbor interactions were included in the Hamiltonian with values taken from spin-wave dispersion measurements[14] for FeF_2, where $J_1=-0.069$ K, $J_2=5.278$ K, and $J_3=0.279$ K. The correlation functions for these three types of neighbors were calculated at each temperature step and averaged over ten different configurations of magnetic spins. Increasing the number of MC steps per temperature step dramatically did not change the results once a minimum number of steps is performed so that the simulation stays in quasistatic equilibrium at each temperature. The proportionality constant between C_m and $d(\Delta n)/dT$ is found[10,11] to be the same in $Fe_{0.93}Zn_{0.07}F_2$ and $Fe_{0.46}Zn_{0.54}F_2$ such that, $AC_m=d(\Delta n)/dT$, where $A=9.17\times10^{-6}$. Our sample $Fe_{0.25}Zn_{0.75}F_2$ is near the percolation threshold concentration and cannot obtain long-range order associated with J_2. However there is short-range order which produces a rounded peak in the C_m data at about $T=23$ K. $d(\Delta n)/dT$ vs T data agree with the C_m data near this peak when the proportionality constant $A=9.17\times10^{-6}$ is used as shown in Fig. 1. However, at low temperature C_m and $d(\Delta n)/dT$ are no longer proportional.

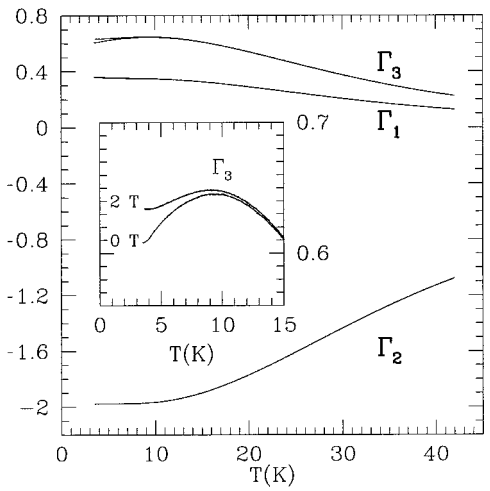

FIG. 2. The first three nearest-neighbor correlation functions $\Gamma_l=\Sigma_{\langle i,j\rangle}\epsilon_i\epsilon_j\langle S_iS_j\rangle_l/N$, where N is the number of sites, versus T for $Fe_{0.25}Zn_{0.75}F_2$ from MC simulations. Note the change in sign of the slope in the $H=0$ T curve at 8 K.

MC simulations provide the opportunity to investigate the relative importance of the different nearest-neighbor interactions on the birefringence. The second-nearest-neighbor interaction dominates the energy Hamiltonian. Therefore the specific heat is dominated by the temperature derivative of the second-nearest-neighbor correlation at the percolation threshold concentration. However, the simulations indicate that $d(\Delta n)/dT$ is significantly governed by the temperature derivative of the third nearest-neighbor correlation. This is evident because the two different correlations have contrasting low-temperature behaviors, with only the third-nearest-neighbor one changing the sign of its slope at low temperature as shown in Fig. 2.

In Fig. 3 we show the MC results for the Ising C_m in the

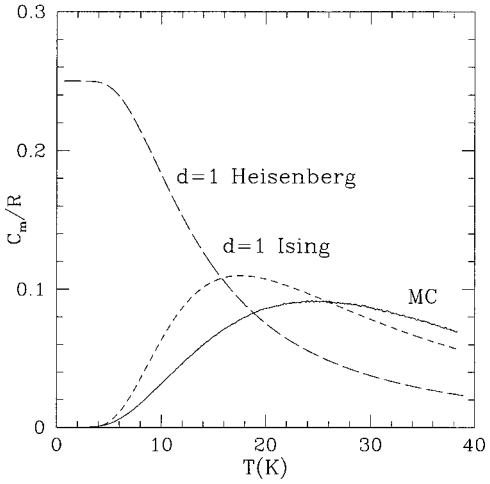

FIG. 3. The magnetic specific heat C_m/R versus T for various models. The C_m per spin predictions have been divided by four in anticipation of a comparison with $Fe_{0.25}Zn_{0.75}F_2$, where the molar specific heat is per Avogadro's number of molecules, which includes the zinc and is four times larger than the number of spins.

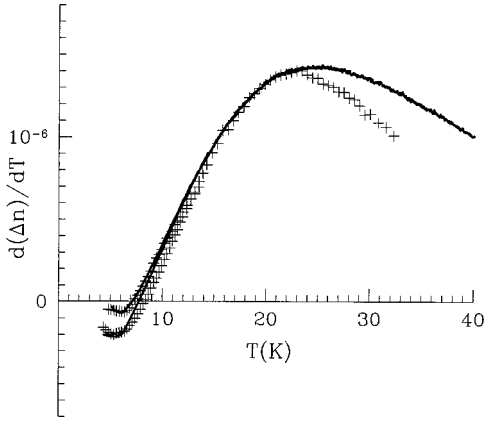

FIG. 5. The temperature derivative of the birefringence $d(\Delta n)/dT$ versus T for $Fe_{0.25}Zn_{0.75}F_2$. Note the change in sign in this $H=0$ T curve at 8 K. The curve through the $H=0$ data is a fit using only the third-nearest-neighbor correlation function from MC simulations with the coefficient I_3 and then scaled by the same factor of 1.5 used to fit the C_m data in Fig. 4. The curve through the $H=2$ T data is the corresponding fit using the third-nearest-neighbor correlation from the $H=2$ T MC simulation.

percolation threshold concentration simulation along with the $d=1$ Ising and Heisenberg exact models. It is reasonable to expect that the $d=1$ Ising model should correspond roughly to the behavior of the simulation. In both systems the spins have an average of two neighbors, there is a similar energy gap and each should have a vanishing specific heat at high temperature. The $d=1$ Heisenberg model, on the other hand, has a finite specific heat at zero temperature (the model is not strictly followed by any real system at low temperature). This comparison does help to explain the fact that the MC data, shown again in Fig. 4 as the small amplitude curve, do not correspond very well to the experimental data. Although the real system has a large anisotropy, it nevertheless has a Heisenberg interaction. While the system exhibits an energy gap and its specific heat falls to zero as the temperature is decreased, a significant amount of specific heat near $T=10$ K is attributable to this Heisenberg interaction. Since we are interested in the relative contributions to the birefringence from the frustrating third nearest interaction, we choose to multiply the pure Ising behavior of the MC data by a factor of 1.5, thereby obtaining the good fit for $T<20$ K exhibited in Fig. 4.

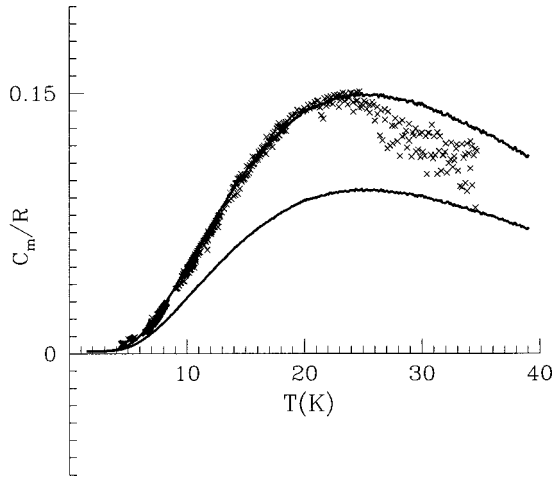

FIG. 4. The magnetic specific heat $C_m/R=C_p/R-B$, where B is the background, versus T for $Fe_{0.25}Zn_{0.75}F_2$. The phonon contribution to the specific heat has been subtracted as discussed in the text. The lower thin line is a fit using only the second nearest-neighbor correlation function from MC simulations. The MC results are then scaled by a factor of 1.5 to obtain a good fit to the experimental data at low temperature.

As mentioned above, at magnetic concentrations $x=0.93$ and $x=0.46$ it has been shown[10,11] that the proportionality between C_m and $d(\Delta n)/dT$ is approximately the same as for pure FeF_2. If we assume the same proportionality for the percolation threshold concentration in the temperature regime where C_m and $d(\Delta n)/dT$ are proportional and that the third nearest-neighbor correlation dominates the behavior of the birefringence, we obtain

$$AJ_2\sum_{i<j}\epsilon_i\epsilon_j\frac{d(\langle S_iS_j\rangle_2)}{dT}=I_3\sum_{i<j}\epsilon_i\epsilon_j\frac{d(\langle S_iS_j\rangle_3)}{dT}. \quad (5)$$

Furthermore, in this temperature regime we expect

$$\sum_{i<j}\epsilon_i\epsilon_j\langle S_iS_j\rangle_2=2\sum_{i<j}\epsilon_i\epsilon_j\langle S_iS_j\rangle_3, \quad (6)$$

where the factor of 2 arises because there are eight second-nearest neighbors and only four third-nearest neighbors. This allows us to calculate I_3 in the previous equation to be 4.85×10^{-5}. With this value of I_3 and the third nearest-neighbor correlation from MC simulations we obtain a good fit to $d(\Delta n)/dT$ at low temperature using the same factor of 1.5 used for C_m, as shown in Fig. 5. We stress that we have calculated I_3 in a regime where C_m and $d(\Delta n)/dT$ are proportional and used this value to fit the simulation results to $d(\Delta n)/dT$, so it is striking that the fit works well below $T=8$ K where C_m and $d(\Delta n)/dT$ are no longer proportional. This provides strong evidence that the third nearest-neighbor correlation dominates the birefringence at low temperature and in the region where C_m and $d(\Delta n)/dT$ are proportional.

However, a small contribution from other correlations can not be ruled out. Detailed fits between the correlations calculated by MC simulation and the birefringence below 8 K suggest such contributions are less than ten percent.

To understand why the small, frustrating third-nearest-neighbor interaction affects the third-nearest-neighbor correlation but has little effect on the second-nearest-neighbor correlation, we turn to the computer simulations. When the simulation is run with only the J_2 interaction included in the Hamiltonian, all three nearest-neighbor correlations have the same temperature dependence as expected. Close inspection of the MC simulation result show that 1.60% of the sites flip at low temperature as a result of the frustration. This is close to the probability of having a site that contains a spin having J_3 interactions but no J_2 interactions which is 1.71%. This suggests that it is the spins that are not dominated by the J_2 interactions that can order via the J_3 interaction. The ordering of these spins is thereby dominated by the J_3 interaction and the temperature derivative of the difference between third-nearest-neighbor correlations calculated with and without the J_3 interaction present shows a typical Schottky peak around a temperature comparable to the interaction strength times average number of neighbors. Since the probability of finding such spins decreases dramatically above the percolation threshold concentration, no such effect should be observed at larger concentrations.

We finally turn to the effect of an applied field on the behavior of $d(\Delta n)/dT$ and hence the third-nearest-neighbor correlations. Having determined the zero-field proportionality between the birefringence data and simulations of the J_3 correlations at low temperature, we can now test whether the same proportionality holds in an applied field even though the correlations themselves change significantly with an applied field at low temperatures. In Fig. 5 we show the measured behavior of $d(\Delta n)/dT$ vs T in an applied field $H=2$ T along the c axis. Also shown in the figure is the MC prediction for the behavior based on the value of I_3 obtained for zero field. The fit is clearly good. Hence the value of I_3 has not changed significantly and the simulation correctly describes the temperature dependence of the birefrincence in the presence of an applied field. This result is important since the birefringence technique has been used extensively[4] to study the RFIM which is realized by applying a field to dilute anisotropic antiferromagnets above the percolation threshold concentration. Near a phase transition the proportionality between C_m and $d(\Delta n)/dT$ holds in a field and the birefringence technique will yield the proper critical behavior. This is important because the birefringence technique invariably yields higher quality data.

We have demonstrated that a small frustrating interaction J_3 affects the corresponding correlation, causing a reversal in the sign of the temperature derivative at temperatures comparable to the interaction strength J_3. In turn, this causes a reversal in the temperature derivative of the birefringence in the case of $Fe_{0.25}Zn_{0.75}F_2$. The behavior of the birefringence in this system is fortuitious because it allows us to determine that third-nearest-neighbor correlation is the dominant one responsible for the birefringence. In most other cases of $d=3$ systems, one cannot determine the source of the birefringence because all the correlations have similar temperature dependences. The fact that the proportionality, given by A, is nearly constant for x between the percolation threshold and pure concentrations in $Fe_xZn_{1-x}F_2$ strongly suggests that the birefringence is dominated by the third-nearest-neighbor correlations for all concentrations. We used the value of J_3 measured for pure FeF_2. The good agreement between the MC simulation and the data suggests that the strength of the frustrating interaction J_3 is close to the same value in the percolation threshold concentration sample. Spin-glass-like behavior[21] near the percolation threshold has strongly hinted at frustration in $Fe_{0.25}Zn_{0.75}F_2$, but the strength of the frustration has not been previously determined. Far above the percolation threshold concentration, or at high temperatures near percolation, this frustrating interaction has little affect on the ordering processes or correlations, which all have the same temperature dependence.

By comparing experimental data for C_m and $d(\Delta n)/dT$ and interpreting the results using MC simulation results, we have been able to explain why the proportionality between C_m and $d(\Delta n)/dT$ fails at low temperature near the percolation threshold concentration but holds at higher temperatures. From the modeling we have done, we have added to the understanding of the origins of the birefringence in the experimental system. We also have shown that the birefringence technique is well behaved even in a field and, as is well documented,[4] the critical behavior of the RFIM is faithfully characterized with the birefringence technique.

This work was funded by Department of Energy Grant No. DE-FG03-87ER45324.

[1] I. R. Jahn, Phys. Status Solidi B **57**, 681 (1973).
[2] J. Ferré and G. A. Gehring, Rep. Prog. Phys. **47**, 513 (1984).
[3] D. P. Belanger, A. R. King, and V. Jaccarino, Phys. Rev. B **29**, 2636 (1984).
[4] D. P. Belanger and A. P. Young, J. Magn. Magn. Mater. **100**, 272 (1991); D. P. Belanger, in *Spin Glasses and Random Fields*, edited by A. P. Young (World Scientific, Singapore, 1998), p. 251.
[5] D. P. Belanger, A. R. King, V. Jaccarino, and J. L. Cardy, Phys. Rev. B **28**, 2522 (1983).
[6] P. Nordblad, D. P. Belanger, A. R. King, V. Jaccarino, and H. Ikeda, Phys. Rev. B **28**, 278 (1983).
[7] I. B. Ferreira, A. R. King, V. Jaccarino, J. L. Cardy, and H. J. Guggenheim, Phys. Rev. B **28**, 5192 (1983).
[8] J. P. Jamet, C. P. Landee, J. Ferré, M. Ayadi, H. Gaubi, and I. Yamada, J. Phys.: Condens. Matter **8**, 5501 (1996).
[9] D. P. Belanger, P. Nordblad, A. R. King, V. Jaccarino, L. Lundgren, and O. Beckman, J. Magn. Magn. Mater. **31-34**, 1095 (1983).
[10] Z. Slaniič and D. P. Belanger, J. Magn. Magn. Mater. **186**, 65 (1998).
[11] K. E. Dow and D. P. Belanger, Phys. Rev. B **39**, 4418 (1989).
[12] P-z. Wong, Phys. Rev. Lett. **77**, 2340 (1996); D. P. Belanger, W. Kleemann, and F. C. Montenegro, *ibid.* **77**, 2341 (1996); R. J.

Birgeneau, Q. Feng, Q. J. Harris, J. P. Hill, and A. P. Ramirez, *ibid.* **77**, 2342 (1996).
[13] D. P. Belanger, Ph.D. thesis, University of California, Santa Barbara, 1981.
[14] M. T. Hutchings, B. D. Rainford, and H. J. Guggenheim, J. Phys. C **3**, 307 (1970).
[15] C. B. de Araujo, Phys. Rev. B **22**, 266 (1980).
[16] A. R. King, I. B. Ferreira, V. Jaccarino, and D. P. Belanger, Phys. Rev. B **37**, 219 (1988).
[17] B. W. Southern, A. P. Young, and P. Pfeuty, J. Phys. C **12**, 683 (1979).
[18] A. C. Lamas and C. P. Landee, J. Appl. Phys. **63**, 3548 (1988).
[19] The crystal was grown by N. Nighman and cut by A. R. King in the laboratory of V. Jaccarino at UCSB.
[20] K. Haefner, Ph.D. thesis, University of Chicago, 1964.
[21] F. C. Montenegro, S. M. Rezende, and M. D. Coutinho-Filho, Rev. Bras. Fis. **21**, 192 (1991).